Boron-doped silicon film as a recombination layer in the tunnel junction of a tandem solar cell*

Shi Mingji(石明吉)†, Wang Zhanguo(王占国), Liu Shiyong(刘石勇), Peng Wenbo(彭文博), Xiao Haibo(肖海波), Zhang Changsha(张长沙), and Zeng Xiangbo(曾湘波)

(Key Laboratory of Semiconductor Materials Science, Institute of Semiconductors, Chinese Academy of Sciences, Beijing 100083, China)

Abstract: Boron-doped hydrogenated silicon films with different gaseous doping ratios (B_2H_6/SiH_4) were deposited in a plasma-enhanced chemical vapor deposition (PECVD) system. The microstructure of the films was investigated by atomic force microscopy (AFM) and Raman scattering spectroscopy. The electrical properties of the films were characterized by their room temperature electrical conductivity (σ) and the activation energy (E_a). The results show that with an increasing gaseous doping ratio, the silicon films transfer from a microcrystalline to an amorphous phase, and corresponding changes in the electrical properties were observed. The thin boron-doped silicon layers were fabricated as recombination layers in tunnel junctions. The measurements of the *I–V* characteristics and the transparency spectra of the junctions indicate that the best gaseous doping ratio of the recombination layer is 0.04, and the film deposited under that condition is amorphous silicon with a small amount of crystallites embedded in it. The junction with such a recombination layer has a small resistance, a nearly ohmic contact, and a negligible optical absorption.

Key words: PECVD; boron-doping; tunnel junction; recombination rate; rectification
DOI: 10.1088/1674-4926/30/6/063001 **PACC:** 6170; 7340E; 8630J

1. Introduction

Tandem solar cells have attracted extensive interest because of their high conversion efficiency and better stability compared to their single junction counterparts. They incorporate one or more tunnel junctions at the interface of n and p type layer of the adjacent top and bottom cells. These tunnel junctions have rectifying properties and will inhibit the carrier transport[1]. In order to fabricate an efficient tandem solar cell, it is important to design and fabricate good n/p junctions that allow very high recombination rates, pass current under reverse bias with a low resistance, have negligible optical absorption, and should be easily integrated into the multijunction deposition process[2, 3].

The transport mechanism in a "tunnel junction" is non-local recombination. In non-local recombination, electrons and holes from different locations tunnel to a defect state and recombine. For non-local recombination, the defect state density in the middle region of the tunnel junction should be high in order to increase the recombination rate. Therefore, intentionally making a thin recombination layer with a high defect state density can improve the tunnel junction carrier transport[4]. In the past, two approaches have evolved for making an effective recombination layer. The first is to insert a thin layer of a wide band gap foreign material[5, 6]. Wide band gap foreign materials have a high optical transparency and are nearly metallic, thus, providing ample carriers for recombination. However, these materials are typically deposited by electron beam evaporation, which is not compatible with the plasma enhanced chemical vapor deposition (PECVD) processing of monolithic tandem solar cells. The second approach is to insert a thin layer of heavily doped amorphous silicon[3]. The advantage of this method is that its technology is compatible with the PECVD processing of monolithic tandem solar cells[4]. It is well known that doping can modulate the microstructures and the optoelectronic properties of the films. It is necessary to investigate the microstructures of p type films with different gaseous doping ratios and their influence on film properties to look for a better material as the recombination layer.

In this work, a series of boron-doped hydrogenated silicon films with different gaseous doping ratios were deposited and investigated by atomic force microscopy (AFM), Raman scattering spectroscopy, and electrical property measurements. Tunnel junctions with a thin recombination layer of different gaseous doping ratios were fabricated and characterized in terms of their *I–V* behavior and transparency spectra. The optimum deposition condition for the recombination layer was found. The tunnel junction with such a recombination layer has the advantages of a small resistance, a near ohmic contact, and a negligible optical absorption.

2. Experimental details

Boron-doped hydrogenated silicon films were deposited in a three-chambered capacitive coupled radio-frequency (RF

* Project supported by the State Key Development Program for Basic Research of China (No. 2006CB202604), the National Natural Science Foundation of China (No. 60576036), and the National High Technology Research and Development Program of China (No. 2006AA05Z 405).

† Corresponding author. Email: shimingji06@semi.ac.cn

Received 13 January 2009, revised manuscript received 11 February 2009

Table 1. Deposition parameters of the n layer and the p layer of the tunnel junctions.

	SiH_4 (sccm)	H_2 (sccm)	B_2H_6 (sccm)	PH_3 (sccm)	Pressure (Pa)	Power (W)	Temp. (°C)
p	1	100	2	0	150	100	200
n	6	48	0	5	250	20	100

of 13.56 MHz) PECVD system. The reaction gases were H_2, SiH_4 (100%), and B_2H_6 (0.5%, diluted by H_2). The hydrogen dilution ratio (SiH_4/H_2) was fixed at 1/100. The gaseous doping ratios (B_2H_6/SiH_4) were 0, 0.01, 0.02, 0.025, 0.03, 0.04, and 0.08, respectively. The technological parameters are selected as follows: an electrode area of 10×10 cm^2, an electrode spacing of 20 mm, a background pressure of 1×10^{-4} Pa, a substrate temperature of 70 °C, an RF power of 100 W, and a reaction gas pressure of 600 Pa. The substrates were glass and quartz wafers for optical and electrical measurements. A hydrogen plasma was used to clean the substrates for 5 min before the film deposition. The surface morphology was measured by using a Solver P47 AFM.

The Raman scattering spectra were tested at room temperature by using a Renishaw-RM-1000. The test system employs an argon ion laser beam (514.5 nm), the spot power density of which is smaller than 100 kW/cm^2 to prevent crystallization of the films. Then coplanar aluminum electrodes were deposited on the samples with a quartz substrate for the measurement of the electrical conductivity. Four tunnel junctions were fabricated to determine the optimum gaseous doping ratio of the recombination layer. Sample A is a standard n/p junction and its structure is "stainless steel/p uc-Si:H/n a-Si:H/ITO". Samples B, C, and D have a recombination layer of different gaseous doping ratios inserted between the n and p layers. Their structures are "stainless steel/p uc-Si: H/p^+ recombination layer/n a-Si: H/ITO", and the gaseous doping ratios of the recombination layer are 0.02, 0.04, and 0.08, respectively. The thicknesses of the recombination layers, the n layers, and the p layers are about 2, 50, and 10 nm respectively. Other deposition parameters are listed in Table 1. Indium tin oxide (ITO) dots (0.07 cm^2) were deposited on the p-layer as the front electrode by a RF magnetron sputtering technique. The current versus voltage characteristics and the transparency spectra of the tunnel junctions were measured.

3. Results and discussion

3.1. Microstructures of the boron-doped silicon films

Figure 1 shows the Raman spectra of the films with different gaseous doping ratios *R*. It can be seen from the figure that the film gradually evolved from microcrystalline silicon to amorphous silicon with increasing *R*. When *R* is low, the film appears to be typical microcrystalline silicon. With increasing *R*, the crystalline peak dies away, while the amorphous peaks become prominent. It is obvious that boron-doping can suppress the formation of microcrystalline silicon and influence the microstructure of the film[7–11].

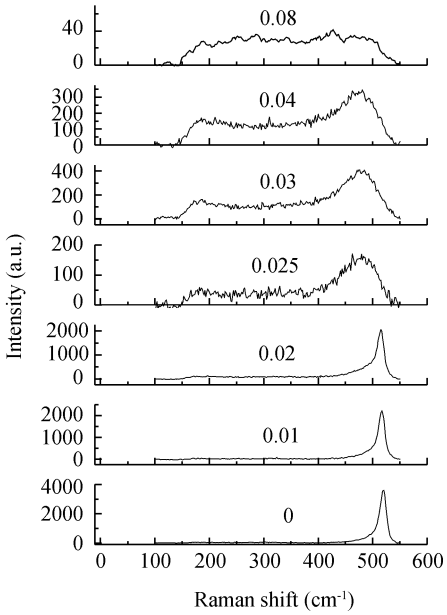

Fig. 1. Raman spectra of the silicon films with different gaseous doping ratios.

Figure 2 shows the AFM morphology images of the films with different gaseous doping ratios *R*. The figure shows that the surface morphology varies with increasing *R*. Yan *et al.*[12] compared conductive-atomic force microscopy (C-AFM) images with AFM morphology images and found that the hill-like structures were clusters formed by aggregated small nanocrystallites, and the flat areas were amorphous regions. We would suppose that the hill-like structures on our sample surface are also clusters formed by aggregated small nanocrystallites. For an undoped film, the surface is densely packed by crystallites with a uniform size of about 50 nm. The crystallites gradually aggregated into clusters with increasing *R* until $R = 0.02$ (in image c), at which point only clusters can be seen. It is worth noting that when *R* increased to 0.025 (in image d), all the clusters disappeared, and a few crystallite appeared on the amorphous silicon background. Subsequently, the amount of the crystallites decreased with increasing *R*. In the last image (in image f), almost the whole film turned into the amorphous phase. This result is consistent with that of the Raman spectra mentioned above.

3.2. Analysis of the electrical properties

Figure 3 shows the room temperature electrical conductivity σ of the films as a function of the gaseous doping ratio *R*. It can be seen that with increasing *R*, the electrical conductivity first increased slightly, then decreased rapidly, followed by a plateau. The *R* dependence of the electrical conductivity can be understood by considering two aspects. One is the effect of

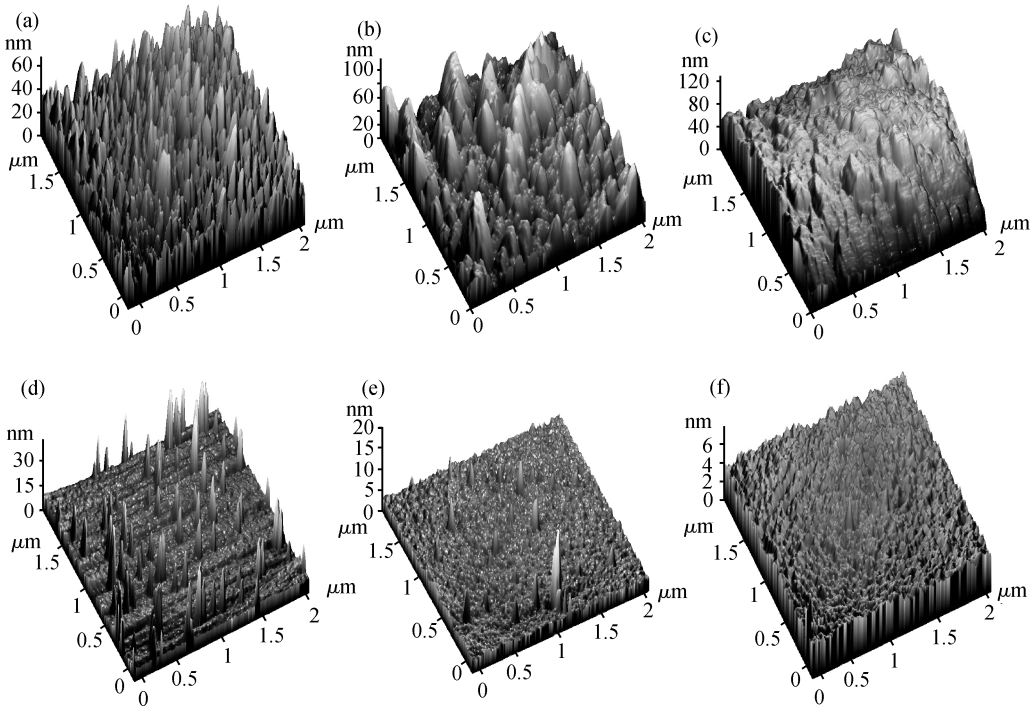

Fig. 2. AFM images of the morphology of the samples with different gaseous doping ratios: (a) 0; (b) 0.01; (c) 0.02; (d) 0.025; (e) 0.04; (f) 0.08.

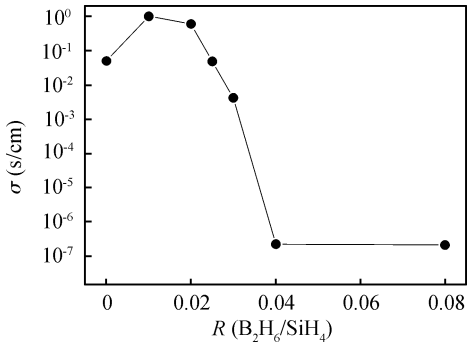

Fig. 3. Electrical conductivity versus *R*.

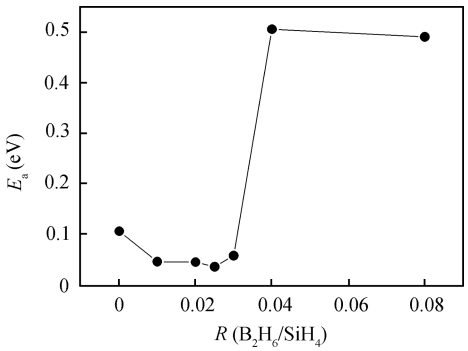

Fig. 4. Activation energy versus *R*.

boron-doping; another is the influence of the microstructure. Boron-doping can increase the carrier density and increase the conductivity; on the other hand, a part of the boron atoms introduced into the silicon network can act as scattering centers and reduce the conductivity[13]. This might be one of the reasons for the complex structure of the σ–R curve. Nevertheless, the dominant factor is most likely the change in the microstructure, as can be seen in Figs. 2 and 3. The sudden drop of the conductivity occurred just where the morphology itself shows a sharp change, which is a transition from microcrystalline to amourphous silicon.

Figure 4 shows the activation energy E_a of the films as a function of R. E_a first decreases, then increases with increasing R. The trend of E_a is consistent with that of the electrical conductivity. The decrease of E_a at the beginning is obviously caused by boron-doping. The sudden rise could be attributed to the transition from microcrystalline to amorphous silicon, where the doping efficiency of boron is much lower than that of microcrystalline silicon, and, consequently, the Fermi level moves back towards the midgap.

In addition, the incorporation of boron atoms might be beneficial to the increase of the concentration of recombination centers, because the dangling bond density is proportional to the square root of the impurity content. In addition, the effect of a distortion in the vicinity of the impurity, caused by the incorporation of a high concentration of atoms with coordination 3, can create Si–Si weak bonds and a certain quantity of dangling bonds[14].

3.3. Fabrication of the recombination layer in the tunnel junction

To find an effective recombination layer for the tunnel junctions, the layer must possess both a small resistance and a high defect density. However, boron-doping has opposite effects on them, so we must find a balance.

A series of tunnel junctions were fabricated. Sample A is a tunnel junction without a recombination layer; samples B, C, and D are tunnel junctions with recombination layers (R = 0.02, 0.04, and 0.08, respectively).

The tunnel junctions were characterized by their I–V curves at room temperature. As shown in Fig. 5, the tunnel junction without a recombination layer does have a rectify-

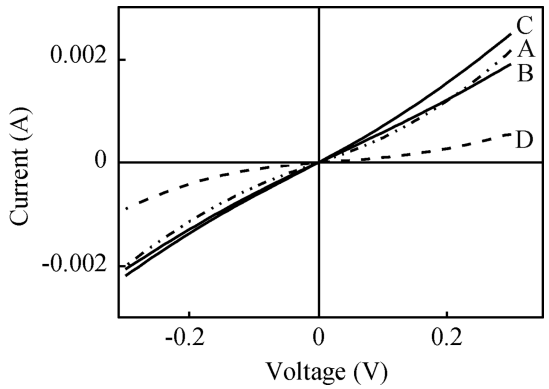

Fig. 5. *I–V* characteristics of the tunnel junctions. Sample A is the standard n/p junction; samples B, C, and D have a recombination layer inserted between the n and p layers. The gaseous doping ratios are 0.02, 0.04, and 0.08, respectively.

ing property. The rectifying effect of the other tunnel junctions depends on the gaseous phase doping ratio. Sample C has the smallest resistance and almost no rectifying effect, offering a nearly ohmic contact. The transparency spectra showed that the absorption losses in the recombination layer are negligible. Therefore, the best gaseous doping ratio of the recombination layer is 0.04. The film deposited under that condition is amorphous silicon with a small amount of crystallites embedded in it.

4. Conclusion

A series of boron-doped hydrogenated silicon films with different gaseous doping ratios R were deposited and investigated by AFM, Raman scattering spectroscopy, and electrical property measurements. With increasing gaseous doping ratios, the silicon films transfer from a microcrystalline to an amorphous phase, and corresponding changes in the electrical properties were observed. The measurements of the *I–V* characteristics and the transparency spectra for the tunnel junction with a recombination layer indicated that the best gaseous doping ratio R is 0.04. The film deposited under that condition is amorphous silicon with a small amount of crystallites embedded in it. The tunnel junction with such a recombination layer has the advantages of a small resistance, a nearly ohmic contact, a negligible optical absorption, and compatible with the multijunction deposition process.

Acknowledgement

The authors wish to acknowledge Professor Guanglin Kong for helpful discussions.

References

[1] Zhu Feng, Zhao Ying, Wei Changchun, et al. Effect of NP tunnel on thin film a-Si/μ-Si tandem solar cells. Journal Synthetic Cryst, 2006, 35(1): 81 (in Chinese)

[2] Kwak J, Kwon S W, Lim K S. Fabrication of a n–p–p tunnel junction for a protocrystalline silicon multilayer/amorphous silicon tandem solar cell. J Non-Crystalline Solids, 2006, 352: 1847

[3] Hegedus S S, Kampas F, Xi J. Current transport in amorphous silicon n/p junctions and their application as "tunnel" junctions in tandem solar cells. Appl Phys Lett, 1995, 67(6): 813

[4] Hou J, Xi J, Kampas F, et al. Non-local recombination in "tunnel junctions" of multijunction amorphous Si alloy solar cells. Mater Res Soc Symp Proc, San Francisco, California, 1994, 336: 717

[5] Sakai Y, Fukuyama K, Matsumura M, et al. The effect of interposing thin oxide layers on the photovoltaic properties of a-Si: H solar cells between the middle n and p layers of a tandem-type cell. J Appl Phys, 1988, 64(1): 394

[6] Shen D, Schropp R, Chatham H, et al. Improving tunneling junction in amorphous silicon tandem solar cells. Appl Phys Lett, 1990, 56(19): 1871

[7] Jiang Xiangliu, He Yuliang, Zhu Hongliang. Neutralization of boron dopants by hydrogen in micro-crystalline silicon films. Chinese Journal of Semiconductors, 1993, 14(11): 664 (in Chinese)

[8] Ji P, De C, Je B, et al. Neutralization of shallow acceptor levels in silicon by atomic-hydrogen. Phys Rev Lett, 1983, 51(24): 2224

[9] Sah C T, Sun Y C, Tzou J J, et al. Deactivation of group III acceptors in silicon during keV electron irradiation. Appl Phys Lett, 1983, 43(10): 962

[10] Wang Jinliang, Xu Gangyi, Wang Tianmin. Study on the microstructures of doped nc-Si: H films. Progress in Natural Science, 2001, 11(3): 331 (in Chinese)

[11] Zhu Feng, Zhao Ying, Zhang Xiaodan, et al. P-nc-Si:H film materials and its application in microcrystalline silicon solar cells. Journal of Optoelectronics· Laser, 2004, 15(4): 381 (in Chinese)

[12] Yan B, Jiang C S, Teplin C W, et al. Local current flow in amorphous and nanocrystalline mixed-phase silicon solar cells. J Appl Phys, 2007, 101(3): 33712-1

[13] Lin Lie, Cai Hongkun, Zhang Dexian, et al. Influence of boron doping on conductivity of amorphous silicon films and photovoltaic efficiency of solar cells. Journal of Optoelectronics· Laser, 2003, 14(11): 1146 (in Chinese)

[14] De Lima M M, Freire F L, Marques F C. Boron doping of hydrogenated amorphous silicon prepared by RF-co-sputtering. Brazilian Journal of Physics, 2002, 32(2): 379